Biological Forum – An International Journal **15(10): 585-592(2023)**

ISSN No. (Print): 0975-1130
ISSN No. (Online): 2249-3239

Geospatial based Land Use Land Cover Change Detection in Jabalpur district, Madhya Pradesh

Jyoti Lohare[1*], Reena Nair[1], S.K. Sharma[2], S.K. Pandey[1] and Shiv Ramakrishnan[3]
[1]Department of Horticulture, College of Agriculture,
J.N.K.V.V., Jabalpur (Madhya Pradesh), India.
[2]Department of Soil & Water Engineering, College of Agricultural Engineering,
J.N.K.V.V., Jabalpur (Madhya Pradesh), India.
[3]Department of Plant Physiology, College of Agriculture,
J.N.K.V.V., Jabalpur (Madhya Pradesh), India.

(Corresponding author: Jyoti Lohare)*
(Received: 29 July 2023; Revised: 30 August 2023; Accepted: 24 September 2023; Published: 15 October 2023)
(Published by Research Trend)

ABSTRACT: For developmental planning and management on sustainable basis of any area mapping and monitoring of land use land cover (LULC) is necessary. For sustainable development of land use land cover to help the planners and policy makers remote sensing and GIS has become a proven tool. This study is an attempt to assess or estimate the change in land use/land cover using remote sensing (RS) and Geographical Information System (GIS) in Jabalpur district, Madhya Pradesh between 2016 and 2022. Sentinel – 2A satellite data for the period has been used to extract LULC using Maximum likelihood supervised classification method. There are five LULC classes were identified in the study area such as agricultural land, built-up land (habitation), open/barren/wasteland, forest, and waterbodies. Results obtained shows increase in built up area and waterbody by 26.70% and 7.88% respectively between 2016 and 2022.

Keywords: Sustainable development, Sentinel.

INTRODUCTION

For gaining continual goals at the juncture of 21st century country is facing several threats like climate change, increasing frequency of disasters which arrests the human progress (Mishra *et al.,* 2020). Anthropogenic activities are responsible for driving these changes which results in modified landscape that affects the ecosystem (Sharma *et al*., 2012; Sharma *et al.,* 2011). Further scientific studies (Liping *et al*., 2018; Rojas *et al.*, 2013; Jianchu *et al*., 2005) supports the argument that landscape changes are notably related with biodiversity losses, degrading water quality, and increased carbon emission. To understand the interaction between the human and environment the landscape change is very important criteria (Patil *et al.*, 2017; Gajbhiye and Sharma 2017). Therefore, land use land cover mapping and change detection is necessary to achieve sustainable developments for human being (Sharma *et al.*, 2016).

Traditional methods of sixties and seventies for LULC mapping were time consuming and error prone (Sharma *et al.,* 2014; Sharma and Seth 2010). In present era satellite image based monitoring of earth surface in the form of LULC map are widely recognized (Abbas *et al.,* 2010; Yang *et al.,* 2012; Subedi *et al.,* 2013; Hassan and Nazem 2015; Li *et al.*, 2016; Lamchin *et al.,* 2018; Shiferaw *et al.,* 2019). Geospatial based LULC change detection techniques have been successfully employed during last decades for whole globe (Jin *et al.,* 2013; Jia *et al.,* 2014; Zhu and Woodcock 2014; Phiri and Morgenroth 2017; Jin *et al.,* 2017; Wu *et al.,* 2018). Globally various researchers effectively determined the various land cover replacement by different LULC categories (Salazar *et al.,* 2015; Duong *et al.,* 2016; Tolessa *et al.,* 2017; Niquisse *et al.,* 2017; Gashaw *et al.,* 2018). For planning and development of any area LULC map is a prerequisite (Tiwari *et al.,* 2017; Lohare *et al*., 2023). LULC has major implication on various issues of earth eco-system like biodiversity, socio-economic vulnerability of people, environmental sustainability etc (Sala *et al.*, 2000). Changes observed in LULC are due to increasing population, industrialization and urbanization. A country like India that supports 17.50 % of world's population on 2% global land areaneeds LULC based change detection studies (Sharma *et al.,* 2018). According to last census (2011) population growth rate of Madhya Pradesh was 20.35 per cent and population of Jabalpur 1268848. Therefore, for developmental planning on sustainable basis spatial mapping and monitoring of LULC is very important to feed the demand of increasing population.

Changes in the state and configuration of land cover have implications on climatic conditions of an area also on living status of people. Due to increase in population and city urbanization, large area of agricultural land and forest covers are being converted into other land uses in Madhya Pradesh resulted in various problems. According to Department of Agriculture and Framers Welfare, Directorate of Economics and Statistics in MP during 2000-01 out of total geographical area (30755361 ha.) of state, area under forest was 28.14 per

cent, fallow land 4.5 per cent, net sown area 47.67 per cent. While, in the year 2020-21 forest 28.3 per cent, fallow land 1.49 per cent, net sown area was 51.31 per cent. However, in Jabalpur district during 2000-01 out of total geographical area (519757 ha.) of district forest 14.40 per cent, fallow land 8.02 per cent, and net sown area was 51.33 per cent. While, during 2020-21 the area under forest 14.93 per cent, fallow land 4.29 per cent and net sown area was 53.75 per cent. So, for sustainable development & planning LULC mapping & change detection is crucial not only for 72.6 Million people of Madhya Pradesh, but also many more people of adjoining states because Madhya Pradesh is a larger grower and production state of cereals, pulses and horticultural crops.

In the present study high resolution (10m) Sentinal-2A Imagery has been used to map the changing pattern of LULC of Jabalpur district from 2016 to 2022. Apart from above all considerations, technological, socio-economic and institutional setup is also inferred to govern the LULC pattern. With the increasing scale of anthropogenic change and impact on environment, it has become important to have land use resources inventory of Jabalpur district. As per census 2011, 41.5 per cent population lives in the rural areas and they are dependent on agriculture. Also, population density from 413 persons per square km in the year 2001 to 2011 has increased to 473 persons per square km, which warrants utilizing resources in judicious manner. So, this again justifies mapping the LULC of the district. There have been some attempts to study the LULC of the district, however very few researchers attempted the change detection study of Jabalpur district using fine resolution satellite data (10m), therefore this paper aims to utilize geospatial technique to detect the LULC changes in Jabalpur district from 2016 to 2022.

MATERIALS AND METHODS

Study area. The present study is conducted in Jabalpur district which is located on the bank of Narmada river and comes under Kymore Plateau and Satpura Hills Agro Climatic Zone (Zone-VII). Its total area is 519757 haand geographically located between 22° 49' 42" N to 23° 37' 5" N and 79° 20' 56" E to 80° 35' 10" E. The district comprises of 1457 villages divided into seven developmental blocks *i.e.*, Jabalpur, Sihora, Majholi, Patan, Shahpura, Panagar and Kundam. The climate of district is favorable for cereals, pulses, oilseed, and horticultural crops with the maximum temperature in May (40-43°C) and minimum in January (8-10°C). Average annual rainfall of the district is 1358 mm. The total irrigated area is 28%. Most of the area of the district is having clay soil (45%) and some of the area contains light soil (25%). Elevation ranges from 325 to 765 m above mean sea level (MSL). Location map of study area is presented in Fig. 1.

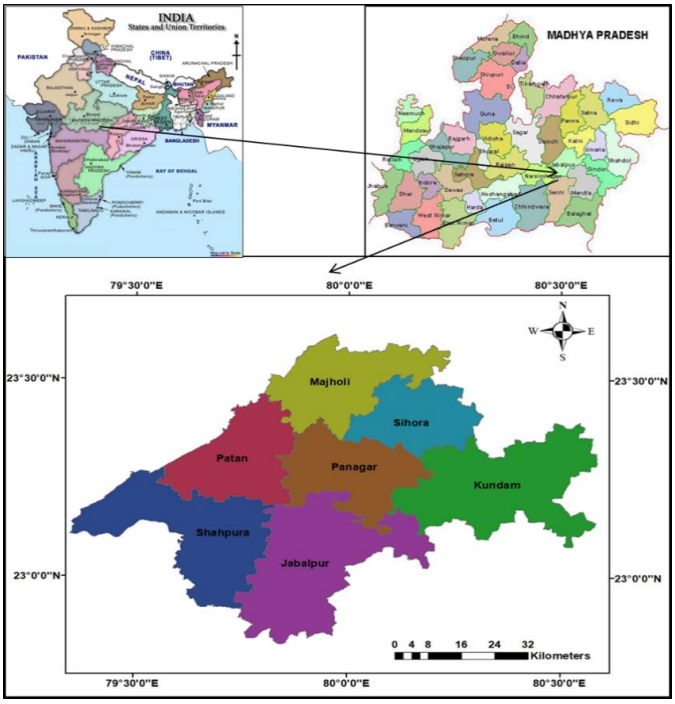

Fig. 1. Location map of study area.

Data source: A cloud free satellite image of Sentinel 2A MSI (Multi Spectral Instrument) with spatial resolution of 10m has been used to prepare the LULC map of the study area. This satellite image was downloaded from Copernicus Open Access Hub website (https://scihub.copernicus.eu/). The date of acquisition of the satellite image was 15th December 2016 (L1C,4 tiles) and 19th December 2022 (L2B, 4 tiles) and a total number of 8 tiles with its tile name as T44QLL, T44QLM, T44QML, T44QMM together coinciding with district boundary were used. The downloaded tiles were having projected coordinate system as UTM Zone 44N and geographic coordinate system as WGS 1984.

The brief information of spatial and spectral characteristics of different band used in Sentinel 2A MSI is presented in Table 1 (Patle *et al*., 2020).

Table 1: Brief details of spatial and spectral characteristics of bands used in Sentinel 2A MSI.

Band	Spatial resolution (m)	Wavelength (µm)	Description
Band 1	60	0.443	Ultra-Blue-Coastal and Aerosol
Band 2	10	0.490	Blue
Band 3	10	0.560	Green
Band 4	10	0.665	Red
Band 5	20	0.705	Visible and Near Infrared (VNIR) – Vegetation Red Edge 1
Band 6	20	0.740	Visible and Near Infrared (VNIR) – Vegetation Red Edge 2
Band 7	20	0.783	Visible and Near Infrared (VNIR) – Vegetation Red Edge 3
Band 8	10	0.842	Near Infrared (NIR)
Band 8A	20	0.865	Narrow Near Infrared (NNIR)
Band 9	60	0.945	Short Wave Infrared (SWIR) – Water Vapour
Band 10	60	1.375	Short Wave Infrared (SWIR) – Cirrus
Band 11	20	1.610	Short Wave Infrared (SWIR)
Band 12	20	2.190	Short Wave Infrared (SWIR)

LULC Classification approach: To generate reflectance files QGIS software has been used to have atmospherically corrected tiles for initial pre-processing technique. The band-2 (blue), band-3 (green), band-4 (red) and band-8 (NIR) as obtained after atmospheric correction were further used to prepare the RGB composite image for each tile. ERDAS (Earth Resources Data Analysis System) IMAGINE® 2020 is used with the help of layer stack tool to prepare a RGB composite image.

The RGB composite tiles were mosaic ked and further made subset by using vector file of Jabalpur district boundary. The change in band combination of RGB composite image successfully yielded FCC (False Colour Composite) image. FCC can be defined as an artificially generated colour image in which the red, green and blue colours are assigned to the wavelength in which they do not belong in nature. The false colour composite image of the study area is shown in Fig. 2.

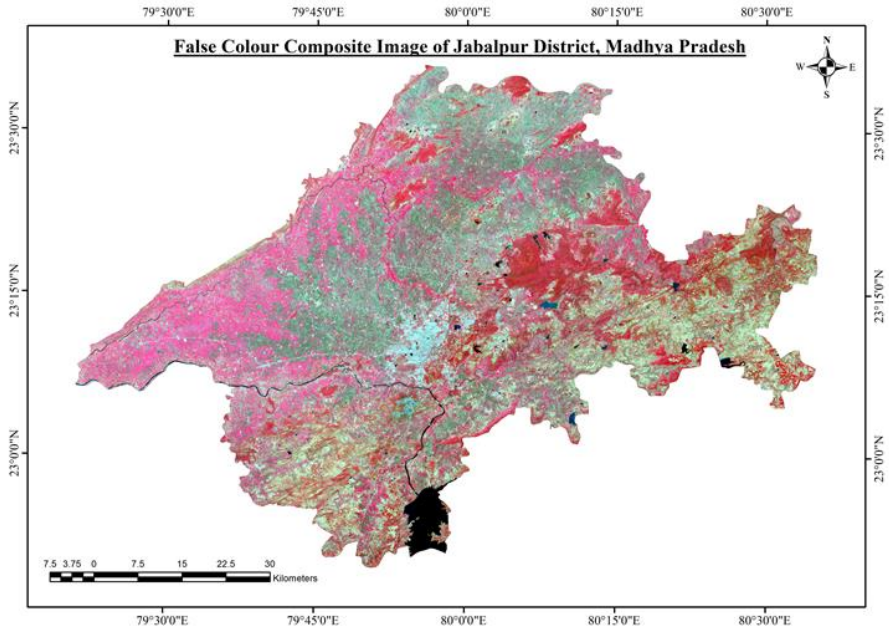

Fig. 2. False Colour Composite image of the study area.

The FCC image of the study area aided in preparing the AOI (Area of Interest) files of different LULC classes using on-screen visual interpretation principles, available ancillary data, prior knowledge-based logic rules, sufficient ground reference data and satellite data of Google Earth Pro. After preparation of AOIs, supervised classification was performed using FCC image that yielded broad classes of LULC in the classified image. The obtained image was recoded to prominent LULC classes characterized by variations in tone, texture, shape, association, and the pattern of various objects within the satellite data.

A total of five prominent LULC classes *viz.*, agricultural land, built-up land (habitation), open/barren/wasteland, forest, and waterbodies were identified during the classification process. Subsequently, the AOI files were further overlaid on supervised classified image to get thematically recoded raster image. At last, area covered by each LULC class was calculated. The methodological framework used in the classification approach is shown in Fig. 3.

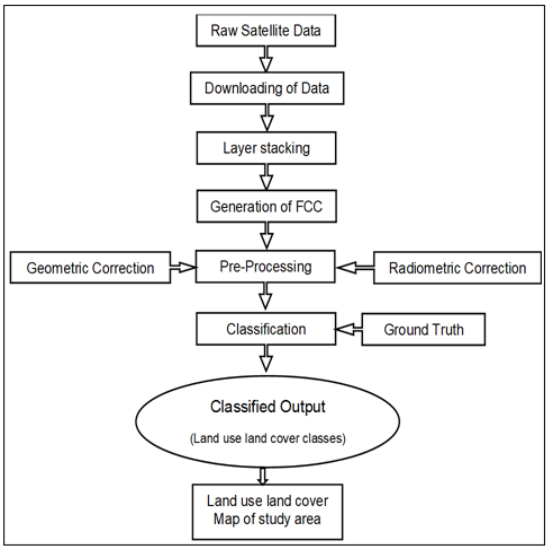

Fig. 3. Methodological framework used in LULC classification approach.

Accuracy Assessment: Accuracy assessment or validation is a significant step in the processing of remote sensing data (Rwanga and Ndambuki 2017). The most common way to express the accuracy of classified image is by a percentage of the map area that has been correctly classified when compared with reference data or "ground truth" (Story and Congalton 1986). This statement can be justified by comparing the correctness of the classification generated by sampling the classified data expressed in the form of an error matrix (sometimes also referred as a confusion matrix or contingency table). An error matrix is a square array of numbers set out in rows and columns, which express the number of sample units assigned to a particular class in one classification relative to the number of sample units assigned to a particular class in another classification (Congalton and Green 2019). The row total in error matrix represents classified data whereas the column total represents reference or ground truth data. An error matrix is a very effective way to represent the accuracy of produced thematic map, because it provides a clear way of deriving the individual accuracies of each class (Congalton and Green 1993).

The error matrix is also used to compute other measures of accuracies such as overall accuracy, producer's accuracy and user's accuracy (Story and Congalton 1986). Producer's and user's accuracies can be computed to determine the individual class accuracies in addition to computing the overall classification accuracy for the entire matrix. The overall accuracy for the image classification can be obtained by dividing the sum of the entries in the "from-to" agreement of the error matrix with the total number of the examined pixels in the classification (Islam *et al.*, 2018). As the name suggests, the producer's accuracy signifies the interest of producer of classification that how well a certain area can be classified (Congalton, 1991). The user's accuracy is indicative of the probability that a pixel classified on the map/image actually represents that category on the ground (Story and Congalton 1986). The error matrix also aides in generating kappa coefficient values which can be used as another measure of agreement or accuracy (Cohen, 1960). The generation of kappa coefficient (k) has become a standard component of almost every accuracy assessment (Rosenfield and Fitzpatrick-Lins 1986; Hudson and Ramm 1987; Congalton, 1991).

For assessing the accuracy of classified map, a total number of 453 randomly distributed points were generated over the entire classified map in ArcGIS® 10.3 environment. The classified data was further compared for agreement with ground truth or reference data obtained from Google Earth Pro satellite data and field visit data.

The post interpretation phase included preparation of LULC maps and detection of their changes. The change detection technique, which was employed in this study, was the post-classification comparison. The overlay consisting of LULC maps of 2016 and 2022 were made through ERDAS IMAGINE software. Then a comparison table was prepared for the overlaid land use/land cover maps of 2016 and 2022.

RESULTS AND DISCUSSION

LULC Classification: The land use land cover classification at large scales (District level) is a heavy computational task yet is critical to landowners, researchers and decision makers enabling them to make informal decisions for varying objectives (Yang *et al.*, 2017). A total of five major LULC classes such as agricultural land (i.e., crop land, agricultural plantation), built-up land (i.e., habitation, rural), open/barren/wasteland (i.e., barren rocky, scrub land), forest (i.e., dense/closed and open category of evergreen forest), and waterbodies (i.e., streams, ponds, and reservoirs) were identified in Jabalpur district.

Fig. 4 and 5 shows the classified LULC map of the study area for 2016 and 2022 respectively. The LULC statistics of Jabalpur district is shown in Table 2. It indicates that major portion of Jabalpur district in 2016 is covered by agricultural land 308018 ha (59.26%), forest 95021.90 ha (18.28%) followed by open/barren/wasteland 93962 ha (18.08%) whereas very small area is covered by waterbodies 13923.80 ha (2.68%) and least area is covered by built up land 8839.91 ha (1.70%). Similarly, in the year 2022 the major portion of Jabalpur district is covered by agricultural land 301990 ha (58.10%), forest 95099 ha (18.30%) followed by open/barren/wasteland 96456.11 ha (18.56%) whereas very small area is covered by waterbodies 15020.50 ha (2.89%) and least area is covered by built up land 11200 ha (2.15%).

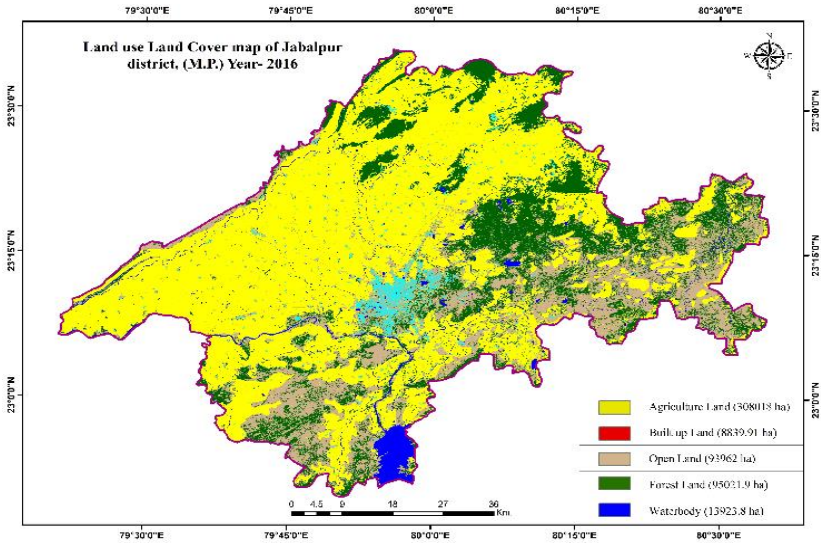

Fig. 4. LULC map of the study area for the year 2016.

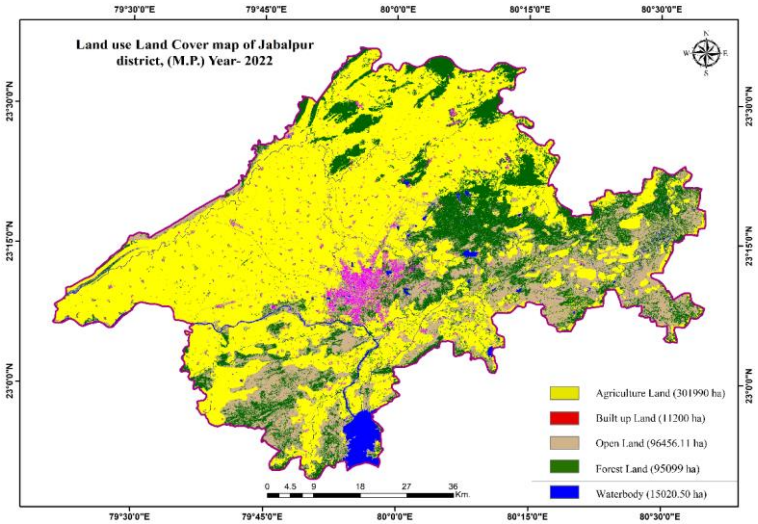

Fig. 5 LULC map of the study area for the year 2022.

Table 2: Comparison of areas and rates of change of the five LULC classes between 2016 and 2022.

LULC Class	2016 LULC Area		2022 LULC Area		Change between 2016 and 2022		Average Rate of change	
	ha	%	ha	%	ha	%	ha/yr	%
Agriculture	308018	59.26	301990	58.10	-6028	-1.96	-1004.67	-0.33
Built-up Land	8839.91	1.70	11200	2.15	2360.09	26.70	393.35	4.45
Open/Barren/ Waste Land	93962	18.08	96456.11	18.56	2494.11	2.65	415.68	0.44
Forest	95021.90	18.28	95099	18.30	77.10	0.08	12.85	0.01
Waterbody	13923.80	2.68	15020.50	2.89	1096.70	7.88	182.78	1.31
Total	519765.61	100	519765.61	100	0.00	0.00	0.00	0.00

It can be observed from Table 2 that study area had been subjected to intensive human influence as the built-up area has increased with 26.70% between 2016 and 2022, water body area has increased to 7.88%, open/barren/waste land has increased to 2.65% least increase (0.08%) observed in forest area for the district. However, agriculture land area is showing 1.96% of decrease from 2016 to 2022.

Table 2 shows the average rate of change per annum for the study area with 4.45% increase in the built up (habitation), 1.31% increase in water body, 0.44% increase in open/barren/waste land, while forest area increase is negligible. However, the decline of agriculture area is meagre i.e. 0.33%.

Accuracy Assessment: To obtain the reliability of classified image, error matrix was generated (Table 3 and 4). The error matrix aided in assessing the overall accuracy, producer's accuracy, user's accuracy and kappa coefficient of the classified map using reference or ground truth data. The overall accuracy of the classified image 2016 and 2022 was found as 88.52% and 93.81% respectively. The producer's accuracy was calculated by dividing the principal diagonal (the agreement) by total number of sample points in that map class as specified by sum of the reference (ground

truth) data (or column total) for that class. Table 3 and Table 4clearly illustrate the process adopted for calculation of producer's accuracy of each class. The computation of producer's accuracy for the year 2016 for different classes of classified image showed that agricultural land producer's accuracy was highest among all the classified classes (96.86%). It was further followed by forest (88.31%), open/barren/waste land (85.36%) and waterbodies (81.81%). The least value of producer's accuracy was obtained for built-up land (25%) indicating a shift in large number of reference data sample points into other classified classes (disagreement) leading to high error of omission. Apart from producer's accuracy, user's accuracy was also calculated for all the produced classes of the classified image. The user's accuracy was highest for waterbodies (100%), followed by agricultural land (91.82%), open/barren/waste land (84.33%), forest (82.92%) and built-up land (70%). The kappa coefficient (k) was found as 0.80.

The computation of producer's accuracy for the year 2022 for different classes of classified image showed that agricultural land producer's accuracy was highest among all the classified classes (i.e., 98.83%). It was further followed by open/barren/waste land (90.56%), forest (89.41%), and waterbodies (81.81%). The least value of producer's accuracy was obtained for built-up land (57.14%) indicating a shift in large number of reference data sample points into other classified classes (disagreement) leading to high error of omission. Apart from producer's accuracy, user's accuracy was also calculated for all the produced classes of the classified image. The user's accuracy was highest for waterbodies (100%), followed by agricultural land (94.79%), open/barren/waste land (92.77%), forest (92.68%) and built-up land (80%). The kappa coefficient (k) was found as 0.89.

A kappa coefficient value of k = 1 indicates a perfect agreement between the categories while a value of k = 0 indicates that the observed agreement equals the chance agreement (Cohen, 1960). A value greater than 0.75 indicates a very good to excellent agreement, while a value between 0.40 to 0.75 indicates a fair to good agreement (Pandey *et al.*, 2007). A value of less than or equal to 0.4 indicates a poor agreement between the classification categories (Manserud and Leemans 1992). On the basis of such criteria, the value of k = 0.94 in this case indicates good to excellent agreement.

The above statements clearly indicate that methodology adopted for satellite image classification to prepare LULC map is satisfactory.

Table 3: Error (Confusion) matrix for the year 2016.

Confusion (Error) Matrix Year-2016 Reference (Ground Truth) Data						
Class Value	**Agriculture**	**Built-up Land**	**Open/Barren/ Waste Land**	**Forest**	**Waterbody**	**Total**
Agriculture	**247**	13	2	6	1	269
Built-up Land	0	**7**	3	0	0	10
Open/Barren/ Waste land	5	5	**70**	3	0	83
Forest	3	3	7	**68**	1	82
Waterbody	0	0	0	0	**9**	9
Total	255	28	82	77	11	**453**

Land Use Land Cover (LULC) Classes	
Agricultural land	AL
Built-up Land	BL
Open/Barren/Waste land	OL
Forest	FT
Water bodies	WB

Overall Accuracy

= {(247+7+70+68+9)/453}×100
= (401/453) ×100
= **88.52%**

Producer's Accuracy	User's Accuracy
AL=(247/255)*100= 96.86%	AL=(247/269)*100= 91.82%
BL=(7/28)*100= 25%	BL=(7/10)*100= 70%
OL=(70/82)*100= 85.36%	OL=(70/83)*100= 84.33%
FT=(68/77)*100= 88.31%	FT=(68/82)*100= 82.92%
WB=(9/11)*100= 81.81%	WB=(9/9)*100= 100%

Kappa coefficient

$$= \frac{(401 \times 453) - (255 \times 269) + (28 \times 10) + (82 \times 83) + (77 \times 82) + (11 \times 9)}{(453)^2 - \{(255 \times 269) + (28 \times 10) + (82 \times 83) + (77 \times 82) + (11 \times 9)\}}$$

= **0.80**

Table 4: Error (Confusion) matrix for the year 2022.

Confusion (Error) Matrix Year-2022 Reference (Ground Truth) Data						
Class Value	**Agriculture**	**Built-up Land**	**Open/Barren/ Waste land**	**Forest**	**Waterbody**	**Total**
Agriculture	**255**	5	2	6	1	269
Built-up Land	0	**8**	2	0	0	10
Open/Barren/ Waste land	3	0	**77**	3	0	83
Forest	0	1	4	**76**	1	82
Waterbody	0	0	0	0	**9**	9
Total	258	14	85	85	11	**453**

Land Use Land Cover (LULC) Classes	
Agricultural land	AL
Built-up Land	BL
Open/Barren/Waste land	OL
Forest	FT
Water bodies	WB

Overall Accuracy

= {(255+8+77+76+9)/453}×100
= (425/453) ×100
= **93.81%**

Producer's Accuracy	User's Accuracy
AL=(255/258)*100= 98.83%	AL=(255/269)*100= 94.79%
BL=(8/14)*100= 57.14%	BL=(8/10)*100= 80%
OL=(77/76)*100= 90.58%	OL=(77/83)*100= 92.77%
FT=(76/85)*100= 89.41%	FT=(76/82)*100= 92.68%
WB=(9/11)*100= 81.81%	WB=(9/9)*100= 100%

Kappa coefficient

$$= \frac{(425 \times 453) - (258 \times 269) + (14 \times 10) + (85 \times 83) + (85 \times 82) + (11 \times 9)}{(453)^2 - \{(258 \times 269) + (14 \times 10) + (85 \times 83) + (85 \times 82) + (11 \times 9)\}}$$

= **0.89**

CONCLUSIONS

This study demonstrated that the recent advances in Remote Sensing and Geographical Information System technologies provide powerful tool for mapping and detecting change in Land Use Land Cover. This research carried out in Jabalpur district, Madhya Pradesh, India using these modern technologies in conjunction with field observations showed both land cover conversion and modifications. The general trend observed by the present study is increase in built up land (habitation) area by 4.45% per annum and very little decrease (0.33%) in agriculture area. The increasing trend of built up area suggest to policy makers to restrict human intervention activities. The findings of the study highlight the need for comprehensive assessment of human activities and the adaptation of suitable measures for the same.

Acknowledgements. The authors are thankful to National Agriculture Higher Education Project (NAHEP), Centre for Advanced Agriculture Science and Technology on "Skill development to use data for natural resources management in agriculture", Department of Soil & Water Engineering, College of Agricultural Engineering, Jawaharlal Nehru Krishi Vishwa Vidyalaya, Jabalpur for providing financial and other support.

Conflict of Interest. None.

REFERENCES

Abbas, I. I., Muazu, K. M. and Ukoje, J. A. (2010). Mapping land use land cover change detection in Kafur local government, Katsina, Nigeria (1995-2008) using remote sensing and GIS. *Res J Environ Earth Sci., 2*, 6-12.

Cohen, J. (1960). A coefficient of agreement for nominal scales. *Educational and Psychological Measurement, 20*(1), 37-46.

Congalton, R. G. (1991). A review of assessing the accuracy of classifications of remotely sensed data. *Remote sensing of Environment*, *37*(1), 35-46.

Congalton, R. G. and Green, K. (1993). Practical look at the sources of confusion in error matrix generation. *Photogrammetric Engineering and Remote Sensing*, *59*(5), 641–644.

Congalton, R. G. and Green, K. (2019). Assessing the Accuracy of Remotely Sensed Data Principles and Practices, Third Edition. In CRC Press.

Duong, P. C., Nauditt, A., Nam, H. and Phong, N. T. (2016). Assessment of climatic change impact on river flow regims in the Red River Delta, Vietnam-a case study of Nhue-Day River basin. *J Nat Resour Dev*, *6*, 81-91.

Gajbhiye, S. and Sharma, S. K. (2017). Prioritization of watershed through morphometric parameters: a PCA based approach. *Appl Water Sci*., *7*(3), 1505-1519.

Gashaw, T., Tulu, T., Argaw, M., & Worqlul, A. W. (2018). Modeling the hydrological impacts of land use/land cover changes in the Andassa watershed, Blue Nile Basin, Ethiopia. *Science of the Total Environment*, *619*, 1394-1408.

Hassan, M. M. and Nazem, M. N. I. (2015). Examination of land use/land cover changes, urban growth dynamics and environmental sustainability in Chittagong city, Bangladesh. *Environ Dev Sustain*, *18*, 9672-9678

Hudson, W. and Ramm, C. (1987). Correct formulation of the kappa coefficient of agreement. *Photogrammetric Engineering and Remote Sensing*, *53*(4), 421-422.

Islam, K., Jashimuddin, M., Nath, B. and Nath, T. K. (2018). Land use classification and change detection by using multi-temporal remotely sensed imagery: The case of Chunati wildlife sanctuary, Bangladesh. *The Egyptian Journal of Remote Sensing and Space Science*, *21*(1), 37-47.

Jia, K., Wei, X., Gu, X., Yao, Y., Xie, X. and Li, B. (2014). Land cover classification using Landsat 8 Operational Land Imager data in Bejing, China. *Geocarto Int*., *29* (8), 941-951.

Jianchu, X., Fox, J., Vogler, J. B., Yongshou, Z. P. F., Lixin, Y., Jie, Q. and Leisz, S. (2005). Land use land cover change and farmer vulnerability in Xishuangbanna Prefecture in Southwestern China. *Environ, Manag*., *36*, 404-413.

Jin, S., Yang, L., Danielson, P., Homer, C., Fry, J. and Xian, G. (2013). A comprehensive change detection method for updating the national land cover database to circa 2011. *Remote Sens Environ*, (132), 159-175.

Jin, S., Yang, L., Zhu, Z. and Homer, C. (2017). A land cover change detection and classification protocol for updating Alaska NLCD 2001-2011, *Remote Sens Environ* (195), 44-55.

Lamchin, M., Lee, W. K., Jeon, S. W., Wang, S. W., Lim, C. H., Song, C. and Sung, M. (2018). Long term trend correlation between vegetation greenness a climatic variable in Asia based on satellite data. *Sci Total Environ*, *618*, 1089-1095.

Li, L., Lu, L. and Kuang, D. (2016). Examining urban impervious surface distribution and its dynamics change in Hangzhou Metroplois. *Remote Sens., 8*, 265

Liping, C., Yujun, S. and Saeed, S. (2018). Monitoring and predicting land use land cover change using remote sensing and GIS techniques-A case study of hilly area, Jiangle, China. *PLoS ONE*, *13*, e0200493.

Lohare, J., Nair, R., Sharma, S. K. and Pandey, S. K. (2023). Review on yield sensing technologies for horticultural crops. *Int. J. Plant Soil Sci., 35* (17), 280-289. Manserud, R. A. and Leemans, R. (1992). Comparing global vegetation maps with the Kappa statistic. *Ecological Modelling*, *62*(4), 275-293.

Mishra, P. K., Rai, A., & Rai, S. C. (2020). Land use and land cover change detection using geospatial techniques in the Sikkim Himalaya, India. *The Egyptian Journal of Remote Sensing and Space Science*, *23*(2), 133-143.

Niquisse, S., Cabral, P., Rodrigues, Â. AND Augusto, G. (2017). Ecosystem services and biodiversity trends in Mozambique as a consequence of land cover change. *Int. J. Biodivers. Sci. Ecosyst. Serv. Manage., 13*, 297–311.

Pandey, A., Chowdary, V. M. and Mal, B. C. (2007). Identification of critical erosion prone areas in the small agricultural watershed using USLE, GIS and remote sensing. *Water resources Management*, *21*(4), 729-746.

Patil, R. J., Sharma, S. K., Tignath, S. and Sharma, A. P. M (2017). Use of remote sensing, GIS and C^{++} for soil erosion assessment in Shakker river basin, India. *Hydrological Sciences Journal*, *62*(2), 217-231.

Patel, D., Rao, J. H. and Dubey, S. (2020). Morphometric analysis and prioritization of sub watershed in Nahara Nala watershed of Balaghat district Madhya Pradesh: A remote sensing and GIS perspective. *Journal of Experimental Biology and Agricultural Sciences, 8*(4), 447-455.

Phiri, D. and Morgenroth, J. (2017). Development in landsat Land cover classification methods: a review. *Remote Sens., 9.*

Rojas, C., Pino, J., Basnou, C., & Vivanco, M. (2013). Assessing land-use and-cover changes in relation to

geographic factors and urban planning in the metropolitan area of Concepción (Chile). Implications for biodiversity conservation. *Applied Geography*, *39*, 93-103.

Rosenfield, G. H., Fitzpatrick-Lins, K. and Ling, H. S. (1982). Sampling for thematic map accuracy testing. *Photogrammetric Engineering and Remote Sensing*, *48*(1), 131-137.

Rwanga, S.S., and Ndambuki, J.M. (2017). Accuracy Assessment of Land Use/Land Cover Classification Using Remote Sensing and GIS. *International Journal of Geosciences*, *8*(04), 611–622.

Sala, O. E., Stuart Chapin, F. I. I. I., Armesto, J. J., Berlow, E., Bloomfield, J., Dirzo, R., ... & Wall, D. H. (2000). Global biodiversity scenarios for the year 2100. *science*, *287*(5459), 1770-1774.

Salazar, A., Baldi, G., Hirota, M., Syktus, J., & McAlpine, C. (2015). Land use and land cover change impacts on the regional climate of non-Amazonian South America: A review. *Global and Planetary Change*, *128*, 103-119.

Sharma, S. K., Gajbhiye, S., Patil, R. J. and Tignath, S. (2016). Hypsometric analysis using Geographical Information System of Gour river watershed, Jabalpur, Madhya Pradesh, India. *Current World Environment. 11*(1): 56-64.

Sharma, S.K., Gajbhiye, S., Tignath, S. and Patil, R. J. (2018). Hypsometric analysis for assessing erosion status of watershed using geographical information system. Hydrological Modeling, Select proceedings ICWEES-2016 (*Springer*), 263-27.

Sharma, S. K., Pathak, R. and Suraiya, S. (2012). Prioritization of sub-watersheds based on morphometric analysis using remote sensing and GIS technique. J.N.K.V.V. *Research Journal*, *46*(3), 407-413

Sharma, S.K**.** and Seth, N. K. (2010). Use of Geographical Information System (GIS) in assessing the erosion status of watersheds. *Sci-fronts A journal of multiple science.* Vol IV**.**

Sharma, S. K., Seth, N. K., Tignath, S. and Pandey, R. P. (2011). Use of Geographical Information System in hypsometric analysis of watershed. *Jour Indian Water Resources Society*, *31*(3-4), 28-32.

Sharma, S. K., Yadav, A. and Gajbhiye, S. (2014). Remote sensing and GIS approach for prioritization of watershed. *LAMBERT Academic Publishing*

Shiferaw, H., Bewlet, W., Alamirew, T., Zeleke, G., Teketay, D., Bekele, K., Schaffiner, U. and Eckert, U. (2019). Implications of land use land cover dynamics and prosopis invasion on ecosystem services values in Afar Region, Ethopia. *Sci Total Environ*, 675, 354-366.

Story, M. and Congalton, R. G. (1986). Accuracy assessment: a user's perspective. *Photogrammetric Engineering and Remote Sensing*, *52*(3), 397-399.

Subedi, P., Subedi, K. & Thapa, B. (2013). Application of a hybrid cellular automaton–Markov (CA-Markov) model in land-use change prediction: a case study of Saddle Creek Drainage Basin, Florida. *Applied Ecology and Environmental Sciences*, *1*(6), 126-132.

Tiwari, J., Sharma, S. K. and Patil R. J. (2017). An integrated approach of remote sensing and GIS for land use and land cover change detection: A case study of Banjar river watershed of Madhya Pradesh. *Current World Environment*, *12*(1), 157-164.

Tolessa, T., Senbeta, F. and Kidane, M. (2017). The impact of land use/land cover on ecosystem services in the central highlands of Ethopia, *Ecosyst. Serv.*, *23*, 47-54.

Wu, T., Luo, J., Fang, J., Ma, J. and Sang, X. (2018). Unsupervised object based change detection via a Weibull mixture model based binarization for high resolution remote sensing images. *IEEE Geosci Remote Sens Lett.*, *15*, 63-67.

Yang, X., Zheng, X., Q. and Lv, L. N. (2012). Spatiotemporal model of land use change based on ant colony optimization, Markov chain and cellular automata. *Ecol Model*, *233*, 11-19.

Yang, D., Fu, C. S., Smith, A. C. and Yu, Q. (2017). Open land-use map: a regional land-use mapping strategy for incorporating Open Street Map with earth observations. *Geo-Spatial Information Science*, *20*(3), 269–281.

Zhu, Z. and Woodcock, C. E. (2014). Continuous change detection and classification of land cover using all available Landsat data. *Remote Sens Environ*., *144*, 152-171.

How to cite this article: Jyoti Lohare, Reena Nair, S.K. Sharma, S.K. Pandey and Shiv Ramakrishnan (2023). Geospatial based Land Use Land Cover Change Detection in Jabalpur district, Madhya Pradesh. *Biological Forum – An International Journal*, *15*(10): 585-592.